Journal of
Micromechanics and
Microengineering

Ultra-precision diamond grinding of vapour cells in silicon for quantum technology

To cite this article before publication: Paul C Gow *et al* 2026 *J. Micromech. Microeng.* in press https://doi.org/10.1088/1361-6439/ae3621

Ultra-precision diamond grinding of vapour cells in silicon for quantum technology

P.C. Gow[1], G.M. Churchill[1], J.W. Thomas[3], B. Steele[2], G. Quick[2], R. Elvin[3], L.J. McKnight[3], C.B.E. Gawith[1], and J.C. Gates[1]

[1]Optoelectronics Research Centre, University of Southampton, Highfield, Southampton, SO17 1BJ, UK
[2]INEX Microtechnology Ltd. Herschel Annexe, King's Road, Newcastle upon Tyne NE1 7RU, UK
[3]Fraunhofer Centre for Applied Photonics, Technology and Innovation Centre, 99 George Street, Glasgow, G1 1RD, UK

E-mail: p.gow@soton.ac.uk

2025

Abstract. We present the use of computer numerical control (CNC) diamond machining with an ultra-precision milling/grinding system to manufacture alkali vapour cells at wafer-scale for quantum technologies. Fabricated cells were loaded with rubidium, bonded under vacuum, and tested in an absorption spectroscopy setup. The results are comparable to similar cells produced via chemical wet etching. Compared to a cleanroom-based chemical etching process, CNC machining can offer a cheaper, more environmentally sustainable route to manufacture of these devices. It also enables rapid prototyping and adjustments to design, whilst simultaneously allowing for scaling to volume production.

1. Introduction

Quantum technologies (QT) such as atomic clocks, gyroscopes, and magnetometers often rely on atomic vapour cells [1]. These cells consist of a volume of an atomic species (typically alkali metals) trapped within a vacuum chamber. Historically these were produced through glass blowing techniques, with an attached stem to allow for active pumping, or for heated pinch-off after cell evacuation [1, 2]. However, this technique is not easily scalable and does not integrate well with the current focus on reducing size, weight, power, and cost of quantum systems towards volume production and commercialization.

Modern techniques for vapour cell production aim to leverage fabrication techniques from the sophisticated field of semiconductor processing, including near-perfect substrate wafers, cleanroom infrastructure, lithography, and material deposition. These routes to production utilise etching and anodic bonding to realise wafer-scale fabrication of atomic vapour cells in silicon [3]. A wafer-scale approach also has the potential for automation, meaning scalable manufacture through automated assembly. Commonly these cells are fabricated by etching of features and through-apertures in a silicon substrate. A layer of borofloat glass is bonded to one side of the wafer. A chemical species in the form of an alkali precursor is then loaded into the cell, and a further piece of glass is bonded under vacuum to enclose the system [4, 5]. Whereas glass-blown cells measure in the range of centimetres, this technique realises vapour cells which measure in the range of millimetres.

An important consideration is maintaining distance between the vapour cloud and the internal surfaces of the cell to allow isolation of the vapour, as well as finding a balance between interaction length, signal to noise ratio, and total cell geometry. This has led to the use of silicon substrates >2 mm thick as a basis for the cell fabrication. However, standard micromachining techniques such as deep reactive ion etching (DRIE) struggle to achieve results in these thicker substrates. Dyer *et al*. demonstrated cells fabricated in 6 mm thick silicon using a waterjet cutter [6]. These showed an improvement in optical signal, however the minimum feature size was limited to 1.5 mm and geometry was restricted to through-holes due to the waterjet limitations. Another way of achieving larger cell geometries is to use a multistack bonding approach. Petremand et. al. employed a multiple layer bonded stack consisting of glass/Si/glass/Si/glass to form a thicker structure [7]. Further to this, Yu et. al. used a novel moulding technique to produce cells in the centre section of the stack with smooth inner walls which allowed multiple angles for optical access and coupling to the cell [8]. Alternatives for improved optical coupling to the cells include utilising reflective sidewalls as mirrors, though the angles of these are restricted to crystal planes by preferential etching [9].

Once sealed, non-evaporable getters (NEGs) can also be employed within the chambers to allow for passive pumping of the cell for improved vacuum. Martinez et. al. employed these alongside multistack bonding and lithographically defined capillaries to produce a Rb beam atomic clock [10]. Once fabricated the vapour cells are activated by employing a laser to release some of the chemical species from the getter pills into the chamber. Maurice et. al. have also demonstrated cells with microfabricated, laser activated 'make' and 'break' seals for activation and sealing of the chambers [11].

Many of these vapour cell designs include 3-dimensional structures, such as wells for storage of atomic species, and vias for transport of atoms to the main chamber. These designs consist of a complex combination of centimeter-length scales, sub-micron precision, and nanometer roughness that is difficult to achieve with standard semiconductor tools. In addition, favoured designs include greater interaction lengths and volumes that must be achieved through thicker materials or multistack bonding, and enhanced optical access through reflective mirrors or optical-quality sidewalls. Thus the fabrication requirements for these devices necessitate the development of novel manufacturing techniques for wafer geometries for them to become commercially viable.

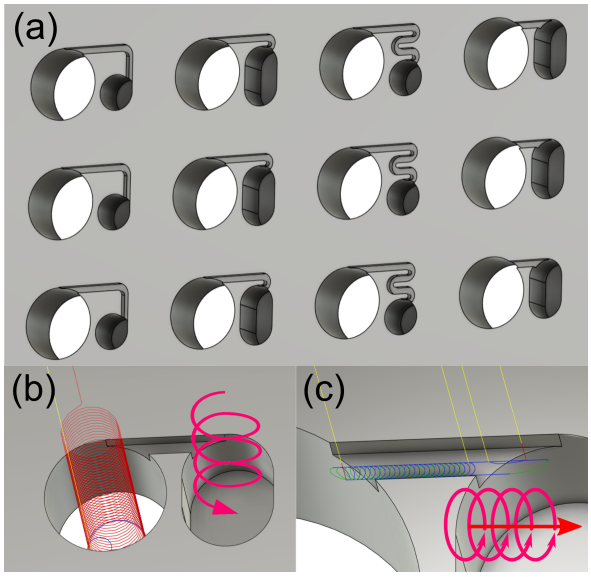

Figure 1. Fig (a) shows a section of the design from Autodesk Fusion360, demonstrating through apertures, blind holes, and different shaped vias for atomic transport. Fig (b) shows the spiral toolpath generated for producing holes, alongside a simplified example. Fig (c) shows the trochoidal toolpath used for machining the vias, alongside a simplified example.

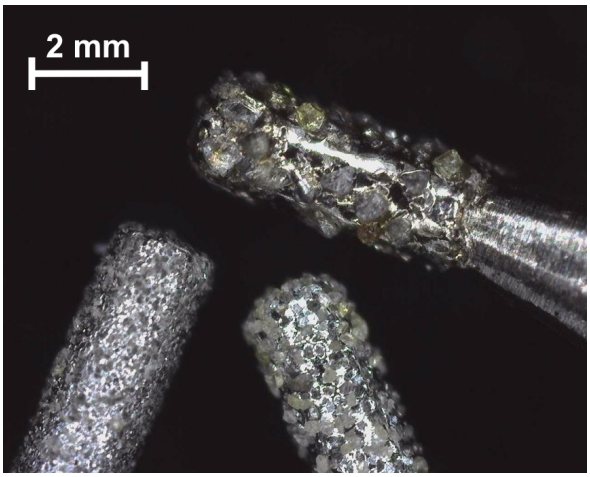

Figure 2. Figure showing three 2 mm diameter diamond superabrasive micro-grinding tools side by side. The different diameters of the diamonds can be seen protruding from the bonding compound.

At Southampton we have machined brittle materials such as; silicon; sapphire; lithium niobate; and glass, to produce optical quality diced waveguides and facets [12], micromilled evanescent refractometers [13], and diced integrated optical fibre cantilevers for sensing [14], as well as producing components for atom/ion trap systems. Apertures are typically used for electrical feed-throughs, vias, and electrical shunts. Such features can be fabricated in silicon and sapphire and utilized for 3D superconductor qubit lattices for quantum computing [15, 16].

Here, we present the application of a Loxham Precision μ6 micromilling system with nanometer precision towards manufacture of components in brittle materials. We present our work on machining atom trap structures in 2 mm thick silicon, both for rapid prototyping of individual dies and at wafer scale for volume production. This method surpasses what is achievable by techniques such as deep reactive ion etching, and is not limited to producing features along crystal planes. This technique is suitable for both rapid prototyping and volume production of 2.5D components for photonics and quantum technology applications.

2. Computer aided design of vapour cells

Use of computer numerical control (CNC) machines for fabrication offer numerous advantages over traditional photolithography techniques for design and rapid prototyping of features and devices. Instead of photomask design and fabrication for lithography techniques, CNC utilises computer aided design (CAD) and computer aided manufacture (CAM) for production of components. Here we use a CAD/CAM package (Autodesk Fusion360) to design, calculate toolpaths, post process, and export code which integrates with the Loxham Precision Ltd μ6 micro turning/milling machine to allow CNC manufacture.

Firstly, a 'blank' of the 2 mm thick, 100 mm diameter silicon wafer was created in the software. Features were then added to this blank to create an array of vapour cells. The basic vapour cell design consisted of a large through-aperture, a well for storage of the alkali precursor pellet, and a small channel between to allow diffusion of the atomic vapour into the main chamber. The wafer featured a total of 104 of each of these features. This featured a variety of layouts, including; through-apertures for vapour trapping ranging in diameter from 2 to 4 mm; blind holes for storage of the alkali precursor measuring 1.4 mm deep; and channels for atom transport measuring 500 μm width. These narrow channels help to suppresses ballistic transport of hot rubidium atoms from the reservoir toward the optical window, forcing motion to be predominantly diffusive. This reduces the flux of Rb reaching the window, minimising the risk of coating and maintaining good transmission over time. It also gives better control of vapour density by acting as a conductance-limiting link, so the interrogation region equilibrates smoothly and is less sensitive to fluctuations in reservoir temperature. The curved channel geometry compounds the advantage by breaking line-of-sight, further reducing contamination and helping maintain a temperature gradient that keeps the metal in the reservoir. Channel design introduces a trade-off between achieving a certain Rb pressure inside the spectroscopy chamber, and reducing the amount of debris from pill activation reaching the main chamber that can weaken the spectroscopy signal. Longer, wider channels with no line of sight, as suggested by Dyer et al., can encourage more Rb to the main chamber whilst limiting activation debris. [6]. Different channel designs, including straight, curved, and S-bend, were used to explore the most ideal design for the transport channels. The cell designs are shown in Fig 1(a).

Next, the diameters of the superabrasive diamond tools (discussed in the following section) were measured on the Loxham machine using its integrated laser toolsetter (Renishaw). The measured diameters were used to create models of the tools within Fusion360 to allow for accurate calculation of toolpaths. Groups of similar sized features (which would require the same diameter tool) were selected within the software and toolpaths were generated. For the apertures a helical toolpath was used, where the tool spirals into the material. This which permits control of the axial material engagement, defining how far the tool moves into the material with each spiral motion. Using tools

smaller than the diameter of the aperture allows for space through which machined material can escape from the aperture. The toolpath used here moves a total of 50 microns into the material for every complete circle. This helical ramp was programmed to begin 50 μm above the material surface for smooth entry into the material. For the through-apertures the machining distance was set to terminate 80 μm past the rear of the wafer to ensure no material was left. As the wafer was mounted on 160 μm thick dicing tape, this additional distance allowed the tool to simply machine into the tape without damaging the mounting chuck or tool. For the 500 μm wide, 500 μm deep channels a trochoidal toolpath was used. This combines a circular and linear toolpath to produce a continuous spiral with small radial engagement along a direction. For this work the overlap distance of the circles was 10 μm. The helical and trochoidal toolpaths are shown in Figures 1(b) and (c) respectively. These toolpaths were post-processed within Fusion360 to produce a file in G-code. This was then exported to the Loxham system and used to machine the features.

3. Ultra-precision micro-grinding of silicon for vapour cell fabrication

Grinding using superabrasive diamond tools is a method commonly employed for lapping and polishing of semiconductor wafers, as well as dicing of these same wafers for singulation of devices. The use of micro-grinding pins allows for machining of features such as holes. Coupled with ultra-precise machines, this allows for good positional control and 2.5D features in brittle materials [17].

A Loxham Precision Ltd μ6 micro turning/milling machine was used for this work. This is a 6-axis CNC machine tool which utilises air-bearing stages with nanometer precision and features an air bearing spindle capable of up to 300,000 rpm. This machine can use standard fluted milling cutters, as well as the diamond micro-grinding tools which are used in this work. The machine also includes a mounted microscope with field of view calibrated to the position of the tool. Therefore optical alignment of the workpiece to existing features such as etched structures or photolithography marks can be performed with micron tolerance. This step is crucial in providing physical machining as a complimentary process to cleanroom techniques. Etching methods such as DRIE can struggle to produce features over 2 mm in depth, and KOH etching typically etches preferentially along the crystal planes of the material, limiting the size, shape, and verticality of features which can be produced. With the on-machine alignment capability it is possible to fabricate these larger shaped features alongside cleanroom processing.

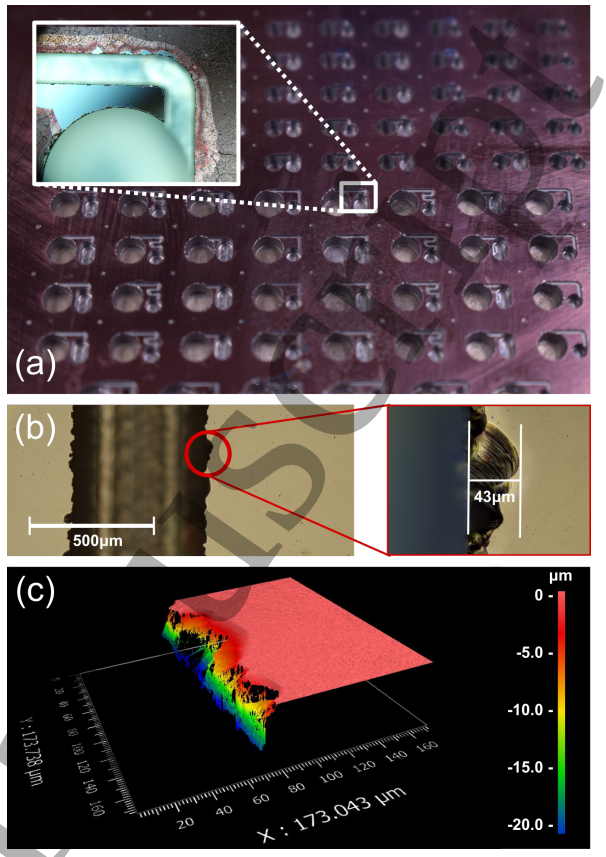

Figure 3. Fig (a) shows the machined wafer with a variety of hole sizes and via shapes. Inset shows a miscroscope image of one of the vias. Some delamination of the photoresist coating is evident, but chipping of the silicon is small and not detrimental to bonding. Fig (b) shows microscope images of one of the larger chips on the wafer, which is less than 50 μm. Fig (c) shows a CSI scan of the chip, showing no burrs which may interfere with later bonding.

A 2 mm thick, 100 mm diameter double-side-polished silicon wafer was used for fabricating the main features of the vapour cells. This was mounted on UV dicing tape and attached to the machine via a vacuum chuck. This method is akin to dicing and allows for easily swapping between machining of single dies or entire wafers. Prior to machining, a coating of photoresist was applied to the surface of the wafer for protection against any scratches induced by removed material. Superabrasive diamond micro-grinding pins were used for machining of the silicon. These have diamond grains of 10's of microns size captured within a sintered metal bonding material, with examples shown in Figure 2. For the large apertures, smaller wells, and channels, tools of 3 mm, 2 mm, and 400 μm diameter were required, respectively. The spindle speeds were 100 krpm for the larger tools and 175 krpm for the smallest. These parameters are summarised in Table 1.

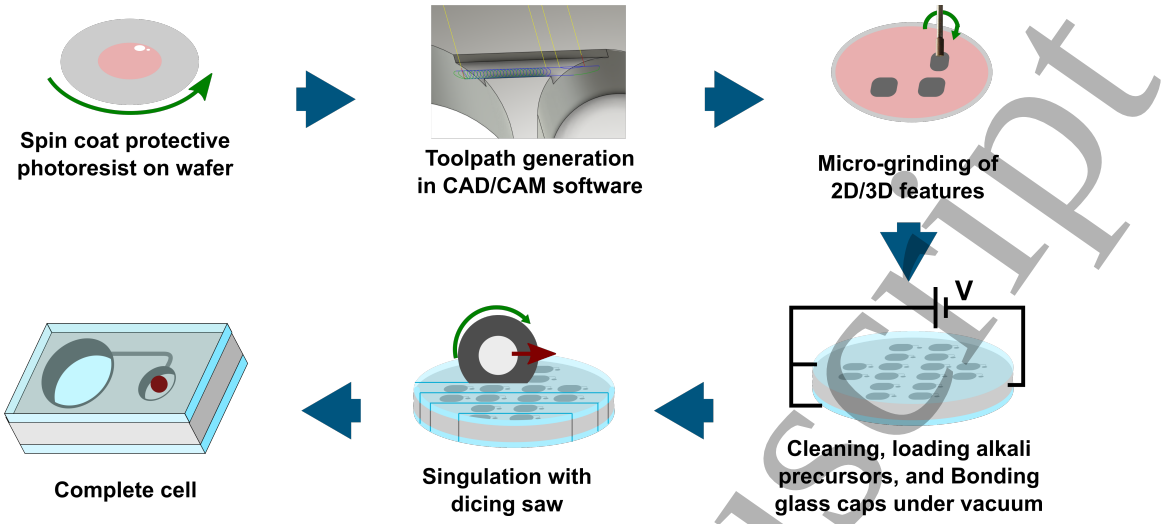

Figure 4. A flow diagram of the manufacturing process. Protection of a 2mm thick silicon wafer is followed by toolpath generation in a CAD/CAM package and micro-grinding. After cleaning, the alkali precursors are added to the wafer and bonding of glass caps is performed under vacuum. The complete wafer is then singulated into individual vapour cells.

The designs drawn in the CAD/CAM software with toolpaths were exported to G-code for the Loxham μ6 to process. Firstly the larger through-apertures were machined, followed by the wells. These features were created using a the helical toolpath discussed in the previous section. The vias between these features were machined with the smallest tools using a trochoidal toolpath. For each of these techniques, the machining feedrates, tool step over, tool grit size, were carefully selected for optimum results. The challenge of physical machining is accuracy and repeatability, which is known as deterministic processing. Vapour cells are relatively tolerant to micron levels of variation; as such, dimensional accuracy was not part of this study. Tool form and tool wear are the primary causes of accuracy and repeatability error. The Loxham Precision μ6 machine features a Renishaw laser tool setter. This provides a measurement of the tool tip position as well as the tool diameter. Frequent tool setting allows tool wear to be taken into account, maintaining good tolerance on depth of cut and machined geometries across the wafer. When wear is excessive, the tool can be changed and machining resumed. In future work we intend to use the on-machine imaging to provide additional inline feedback.

Table 1. A table summarising the tooling, speeds, and paths for machining the vapour cell features.

Tool Diameter (*mm*)	*Spindle Speed* (*kRPM*)	*Grit Size* (μm)	*Tool Path*	*Stepover* (μm)
3	100	40	Helical	50
2	125	40	Helical	50
0.4	175	36	Trochoidal	10

Typically for a uniform, low roughness result when machining brittle materials such as silicon, a shallow depth of cut and slow feedrate is required to ensure chip thickness remains below the critical depth. This allows for machining with little to no chips or cracks and can result in a optical-quality surface finish. Such results, however, are time consuming to achieve due to the low material removal rate. For a technique to have commercial viability, it must have a reasonably high rate of throughput for device creation, balancing cost and performance. An optical quality surface finish was not necessary for these devices. Only low surface chipping to allow for anodic bonding to the silicon surface later. Therefore feed rates and machining depths were optimised for fast processing times with acceptable levels of chipping. In this case, chipping of size less than 50 μm was assumed to be acceptable as this did not significantly reduce the area reserved for bonding. Part of the resulting machined wafer is shown in Figure 3(a), with the inset showing a close up of one of the machined designs. Microscope images of one of the larger chips are shown in Fig.3 (b). Aside from chipping, burrs can also introduce issues for bonding. However, no burrs were evident after micro-grinding of the wafer. Fig.3 (c) shows a coherent scanning interferometer (Zygo Zegage Pro HR) image of this chip, demonstrating that there are no burrs present which may affect the bonding later.

For producing these types of features in a silicon substrate, photolithography or DRIE would be a preferred route to manufacture. However, DRIE can struggle with substrate thicknesses over 2 mm,

therefore the scalability of machining processes for these thicker substrates are of interest. The machined wafer consisted of 104 cells, each featuring large through-apertures, small wells for storage of chemical species, and vias of differing design. Complete with tool changes, the machining time for this 2 mm thick wafer was approximately 26 hours, although this could be reduced through further development of tooling, feedrates etc. For comparison with the machined cells, several vapour cells were manufactured at INEX Microtechnology Ltd via KOH wet etching. This process took up to 5 days to perform the multiple lithogrpahy and etching steps necessary for the different features. With an average etch rate for Si in KOH of 1 μm per minute, the etching step itself is ~30 hours. However, etching can be performed in batches and can be extremely repeatable. Using a dry etching process such as DRIE to produce these features is also possible. Etching rates can be up to tens of microns per minute. However, these rates are highly dependent on crystal axis orientation and total etch depth. With etching methods struggling with depths greater than 2 mm, scaling to thicker cell structures would be difficult. Whilst high throughput can be achieved in wet-etching by batch processing, physical CNC machining can be parallelised by running multiple machines 24 hours a day. Combined with automated pick and place for exchanging wafers and machined devices, and tool wear monitoring with automatic tool replacement, this would allow for high throughput manufacture.

The use of an abrasive machining process as an alternative to cleanroom processing can significantly impact environmental sustainability for the manufacturing of components for deployable quantum technologies [18]. Others have studied typical life-cycle assessments of precision machining processes, considering the life cycle from extraction of raw materials through to product recycling or final disposal [19, 20]. Manufacturing process based around a single machine will have inherent efficiency improvements in power consumption, waste, and environmental sustainability when compared to cleanroom and polishing facilities. Information provided by Loxham Precision indicates that the μ6 machine uses a single-phase wall plug, which typically draws a maximum of 400 W for the translation stages and control systems. The system employs a chiller, with a typical cooling power of around 500 W. Additionally the system requires a supply of compressed air and water supply for coolant. Toolpaths are created through computer aided design (CAD) for each feature, allowing for simple prototyping or alterations to designs without creating new photomasks. Removing the necessity for an energy-hungry facility such as a cleanroom and supporting infrastructure, as well as processing requirements (chemicals, mask creation, waste materials etc) [21], takes a significant step towards reducing the energy requirement for the manufacture of components. As such, micro-grinding can provide a complimentary (or alternative) process for existing cleanroom techniques for manufacture of novel quantum devices, whilst allowing for higher precision than methods such as water jet cutting.

4. Bonding and testing of cells

The machined Si substrate was bonded to form vapour cells in-house at INEX Microtechnology, alongside their etched devices. Firstly, a 0.5 mm thick Borofloat33 glass wafer was bonded onto one side of the machined 2 mm silicon substrate. Anodic bonding was performed using a 600 V source, at a temperature of 300 °C. Next, the blind reservoir holes in the Si were loaded with SAES Rubidium getter pills to act as the alkali precursor. Another 0.5 mm thick Borofloat33 wafer was bonded on to the Si sealing the vapour cells. This final bond was performed under a vacuum of 1e-5 mbar to evacuate the cells, with the resulting bonded wafer shown in Figure 5(a). This resulted in an anodic bonded triple stack of BF33 glass/Si/BF33

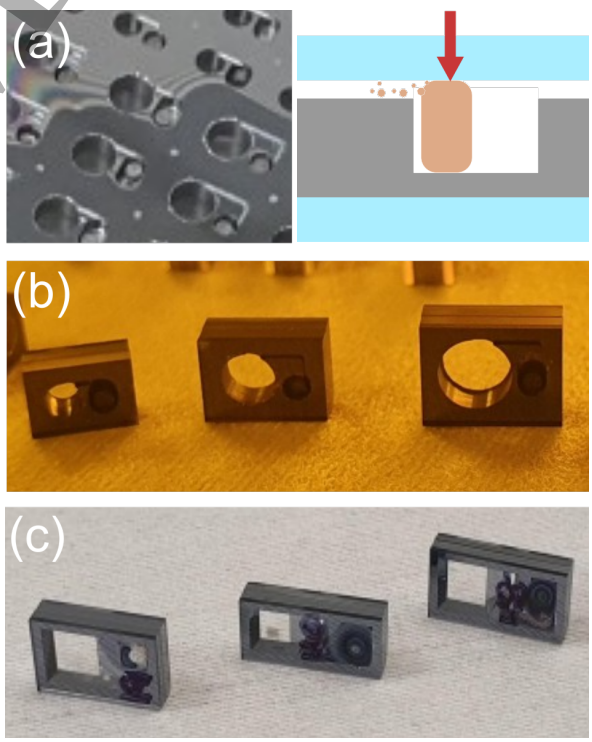

Figure 5. (a) shows an image of the bonding failure caused by a RB loading error. *Left* : The lower half of the area has bonded, whilst the upper half has failed to bond. *Right* : A schematic of the Rb loading error preventing bonding. (b) is an image of the resulting cells manufactured by microgrinding at Southampton. (c) shows the resulting cells fabricated through etching at INEX.

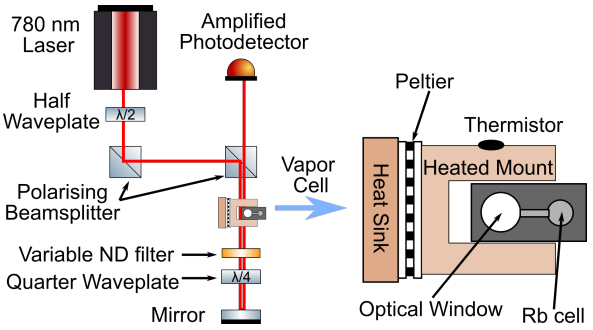

Figure 6. Schematic of the setup for saturated absorption spectroscopy measurements. Exploded view shows a close up of the heater mounting arrangement for the compact cells produced by physical machining, and by etching. This is replaced by a glass-blown reference cell with no heating for comparison.

glass. During loading of the 104 Rb pills into the wafer a manual handling error occurred, resulting in some pills tilting sideways and becoming crushed. This introduced dust between the silicon and glass capping layer and prevented bonding. This is shown in Figure 5(a), alongside a schematic demonstrating the manual handling error. This issue could be improved by automating the dispense with a pick-and-place system. After bonding the 3 mm thick wafer assembly was diced using a Loadpoint MicroAce Series 3 dicing saw. 1.5 mm deep grooves were diced from both sides of the assembly and aligned to the machined holes to singulate the individual cells. This design allows for a 1 mm wide frame around the machined features to promote a strong Si-glass bond area, while minimising total cell size. A flow diagram of the complete fabrication process for the cells is shown in Figure 4, and the resulting machined and etched cells are shown in Figures 5(b) and (c) respectively.

The process yield of the machined cells was low, providing ∼20 useful cells for 104 manufactured on the wafer. This was primarily due to the loading error of some of the Rb pills which prevented bonding (Figure 5(a)). Another reason for cell failure may be a result of the small (1 mm) bonding area allowed in the original design. Subsequent work has shown that increasing the bond area from 1 mm to 1.5 mm can result in an improved, more resilient bond whilst maintaining a small form factor. Edge chipping of the silicon was not believed to restrict bonding as no upward projecting burrs were apparent in any machined structures due to the brittle nature of the material. Unfortunately no cells featuring the serpentine S-bend channels survived the bonding process, so a direct comparison of all channel geometries was not possible.

Both the machined and etched cells were tested at Fraunhofer UK using the setup shown in Figure 6 and compared to a Rb reference cell (Thorlabs GC19075-RB). Firstly, the Rb getter pill was activated via ablation using a high power laser (>1 W). Once activated, Rb propagates through the narrow 500 μm channels to the main window chamber where the vapour is accessible to laser beams. A 780 nm DBR laser source (Thorlabs DBR780PN) was used for the absorption tests, collimated to a beam diameter of 1.5 mm ($1/e^2$) and with power controlled via a half-waveplate and polarizing beam-splitter. Doppler-free saturated absorption spectroscopy was performed by first saturating the cell with 200 μW of pump power. The light was then retroreflected and attenuated to 15 μW via a variable neutral density filter. This was then detected by a Si switchable gain detector (Thorlabs PDA36A2). Both the KOH etched and machined cells were heated to 60 °C such that laser absorption over the 2 mm path length was equivalent to the glass-blown cell measured at 25 °C with a path length of 71.8 mm. This heat was primarily applied to the main window chamber of the cells, to prevent Rb condensation on the windows and provide a temperature gradient towards the reservoir end of the cell. The absorption spectroscopy results are shown in Figure 7.

The results from the machined cells are comparable to measurements from the etched cells of the same path length. Both types of cell showed good sealing, though Rb condensation on the inside of the windows meant the cells required heating to keep the optical path clear. Compared with the commercially available glass-blown cell, both the etched and machined cells exhibited weaker saturated peaks. This is attributed to the possible introduction of a small amount of residue during getter pill activation, the results of which would be much more obvious in smaller volume cells. The saturated spectroscopy height was calculated for two of the larger crossover transitions in each line. For 85Rb, the F = 3 to F' = 3,4 peak was chosen and for the 87Rb line, the F = 2 to F' = 2,3 crossover peak was chosen. The depth was calculated as a percentage of the maximum, and the height of the Doppler-free peak as a fraction of the dip height was calculated. This relative saturation-specific heights for the machined, etched, and reference cells were 27.34%, 27.05%, and 27.72% respectively for the 85Rb line, and 44.33%, 41.14%, and 45.28% for the 87Rb line.

Overall the performance of the machined cells were comparable to those with similar dimensions that were manufactured via etching. The miniature cells were compared to a commercial, glass-blown 71.8 mm Rb cell. To reach comparable absorption depths with a much shorter interaction length, the wafer cells were heated to approximately 60 °C. This required up to 2 W power. The low volume and mass manufacturability the wafer cells, combined with a relatively low power consumption, offers a good solution in portable quantum sensing. The requirement of heating to

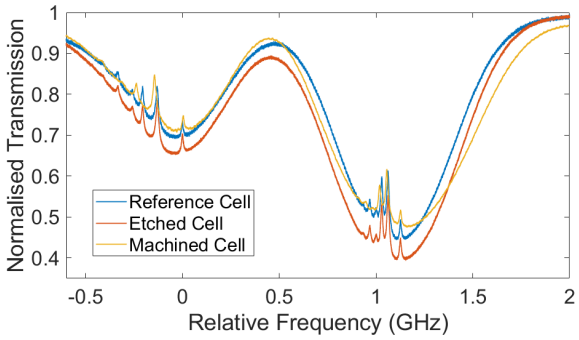

Figure 7. Plot of transmission Data of cells against relative frequency in GHz. The commercially available reference cell, etched, and machined cells show comparable strength of peaks.

60 °C for a strong signal could be readily addressed by increasing the optical path length to reduce the temperature requirements. The advantage of physical micro-grinding of the cell designs is that cells with much longer path lengths could be machined in thicker Si substrates with high precision features. Such dimensions would be difficult, if not impossible, to produce through typical cleanroom microelectronic techniques or water jet cutting. CNC micro-grinding also allows for design changes to be rapidly applied, permitting fast prototyping and scaling for production.

5. Conclusion

This work demonstrates the viability of CNC machining with an ultra-precision milling/grinding system for manufacture of alkali vapour cells at wafer-scale. A variety of features including through-apertures, wells, and vias were created in a CAD/CAM package, and toolpaths were generated. Micro-grinding was performed with superabrasive diamond tools before the resulting machined wafer was loaded with precursor material and bonded under vacuum. Individual cells were then singulated from the bonded stack with a standard dicing saw. Generation of features and toolpaths in a CAD/CAM software allows for rapid prototyping and adjustments to design, whilst simultaneously allowing for scaling to volume production. Compared to a cleanroom-based chemical etching process, CNC machining can offer a cheaper, more environmentally sustainable route to manufacture of these devices. Additionally, feature geometries are not limited as in KOH wet-etching where the substrate preferential etches along crystal planes, and processing of thicker substrates than can be etched with DRIE is also possible. Further work will be towards fabrication of devices in thicker substrates (>4 mm thick), optical grade micro-grinding in glass for transparent material stacks, and ductile machining of silicon to fabricate integrated mirrors within cells.

Funding

Innovate UK grant 50414 (QT Assemble). Royal Academy of Engineering Research Chair (RC-SRF1718639). Engineering and Physical Sciences Research Council grants EP/M013243/1 and EP/T001062/1.

Data Availability

All data supporting this study are openly available from the University of Southampton repository at https://doi.org/10.5258/SOTON/D3761.

References

[1] J. Kitching. Chip-scale atomic devices. *Applied Physics Reviews*, 5(3), 2018.

[2] S. Knappe, V. Velichansky, H. G. Robinson, L. Liew, J. Moreland, J. Kitching, and L. Hollberg. Atomic vapor cells for miniature frequency references. In *IEEE International Frequency Control Symposium and PDA Exhibition Jointly with the 17th European Frequency and Time Forum, 2003. Proceedings of 2003*, pages 31–32. IEEE, 2003.

[3] X. Wang, M. Ye, F. Lu, Y. Mao, H. Tian, and J. Li. Recent progress on micro-fabricated alkali metal vapor cells. *Biosensors*, 12(3):165, 2022.

[4] L-A. Liew, S. Knappe, J. Moreland, H. Robinson, L. Hollberg, and J. Kitching. Micromachined alkali atom vapor cells for chip-scale atomic clocks. In *17th IEEE International Conference on Micro Electro Mechanical Systems. Maastricht MEMS 2004 Technical Digest*, pages 113–116. IEEE, 2004.

[5] L-A. Liew, S. Knappe, J. Moreland, H. Robinson, L. Hollberg, and J. Kitching. Microfabricated alkali atom vapor cells. *Applied Physics Letters*, 84(14):2694–2696, 2004.

[6] S. Dyer, P. F. Griffin, A. S. Arnold, F. Mirando, D. P. Burt, E. Riis, and J. P. McGilligan. Micromachined deep silicon atomic vapor cells. *Journal of Applied Physics*, 132(13), 2022.

[7] Y. Pétremand, C. Affolderbach, R. Straessle, M. Pellaton, D. Briand, G. Mileti, and N. F. De Rooij. Microfabricated rubidium vapour cell with a thick glass core for small-scale atomic clock applications. *Journal of Micromechanics and Microengineering*, 22(2):025013, 2012.

[8] M. Yu, Y. Chen, Y. Wang, X. Han, G. Luo, L. Zhao, Y. Wang, Y. Ma, S. Lu, P. Yang, Q. Lin, K. Wang, and Z. Jiang. Microfabricated atomic vapor cells with multi-optical channels based on an innovative inner-sidewall molding process. *Engineering*, 2023.

[9] R. Han, Z. You, F. Zhang, H. Xue, and Y. Ruan. Microfabricated vapor cells with reflective sidewalls for chip scale atomic sensors. *Micromachines*, 9(4):175, 2018.

[10] G. D. Martinez, C. Li, A. Staron, J. Kitching, C. Raman, and W. R. McGehee. A chip-scale atomic beam clock. *Nature Communications*, 14(1):3501, 2023.

[11] V. Maurice, C. Carlé, S. Keshavarzi, R. Chutani, S. Queste, L. Gauthier-Manuel, J-M. Cote, R. Vicarini, M. Abdel Hafiz, R. Boudot, and N. Passily. Wafer-level vapor cells filled with laser-actuated hermetic seals for integrated atomic devices. *Microsystems & Nanoengineering*, 8(1):129, 2022.

[12] L. G. Carpenter, S. A. Berry, and C. B. E. Gawith. Ductile dicing of linbo3 ridge waveguide facets to achieve 0.29 nm surface roughness in single process step. *Electronics letters*, 53(25):1672–1674, 2017.

[13] L. G. Carpenter, P. A. Cooper, C. Holmes, C. B. E. Gawith, J. C. Gates, and P. G. R. Smith. Nanoscale roughness micromilled silica evanescent refractometer. *Optics express*, 23(2):1005–1014, 2015.

[14] C. Holmes, A. Jantzen, A. C. Gray, L. G. Carpenter, P. C. Gow, S. G. Lynch, J. C. Gates, and P. G. R. Smith. Integrated optical fiber-tip cantilevers. *IEEE Sensors Journal*, 17(21):6960–6965, 2017.

[15] P. A. Spring, S. Cao, T. Tsunoda, G. Campanaro, S. Fasciati, J. Wills, M. Bakr, V. Chidambaram, B. Shteynas, L. Carpenter, P. C. Gow, J. C. Gates, B. Vlastakis, and P. J. Leek. High coherence and low cross-talk in a tileable 3d integrated superconducting circuit architecture. *Science Advances*, 8(16):eabl6698, 2022.

[16] N. Acharya, R. Armstrong, Y. Balaji, K. G. Crawford, J. C. Gates, P. C. Gow, O. W. Kennedy, R. D. Pothuraju, K. Shahbazi, and C. D. Shelly. Integration of through-sapphire substrate machining with superconducting quantum processors. *Advanced Materials*, 37(9):2411780, 2025.

[17] P. C Gow, G. M. Churchill, C. B. E. Gawith, and J. C. Gates. Ultra-precision CNC for the manufacture of components for quantum technologies. In *50th International Micro and Nano Engineering Conference*, 2024.

[18] JC Aurich, B Linke, M Hauschild, M Carrella, and B Kirsch. Sustainability of abrasive processes. *CIRP Annals*, 62(2):653–672, 2013.

[19] ISO Norm. 14040,"life cycle assessment: principles and framework,". *Environmental management*, 2006.

[20] Frank Schneider, Jayanti Das, Benjamin Kirsch, Barbara Linke, and Jan C Aurich. Sustainability in ultra precision and micro machining: A review. *International Journal of Precision Engineering and Manufacturing-Green Technology*, 6(3):601–610, 2019.

[21] Jared M Levy, Michael M Ohadi, and Choo Kyosung. Energy analysis of cleanrooms in an academic research building. *ASHRAE Transactions*, 121(2):71–84, 2015.